Insect Biochemistry and Molecular Biology 54 (2014) 61–68

Contents lists available at ScienceDirect

Insect Biochemistry and Molecular Biology

journal homepage: www.elsevier.com/locate/ibmb

Mode of action of allatostatins in the regulation of juvenile hormone biosynthesis in the cockroach, *Diploptera punctata*

Juan Huang [a], Elisabeth Marchal [a, b], Ekaterina F. Hult [a], Sven Zels [b], Jozef Vanden Broeck [b], Stephen S. Tobe [a, *]

[a] Department of Cell and Systems Biology, University of Toronto, Toronto, Canada
[b] Department of Biology, Zoological Institute, KU Leuven, B-3000 Leuven, Belgium

ARTICLE INFO

Article history:
Received 24 July 2014
Received in revised form
27 August 2014
Accepted 2 September 2014
Available online 10 September 2014

In memory of Dr. Grahame E. Pratt who died on March 8, 2014

Keywords:
Allatostatin receptor
Diploptera punctata
G protein-coupled receptors
Juvenile hormone
RNA interference

ABSTRACT

The FGLamide allatostatins (FGL/ASTs) are a family of neuropeptides with pleiotropic functions, including the inhibition of juvenile hormone (JH) biosynthesis, vitellogenesis and muscle contraction. In the cockroach, *Diploptera punctata*, thirteen FGLa/ASTs and one allatostatin receptor (AstR) have been identified. However, the mode of action of ASTs in regulation of JH biosynthesis remains unclear. Here, we determined the tissue distribution of *Dippu-AstR*. And we expressed Dippu-AstR in vertebrate cell lines, and activated the receptor with the Dippu-ASTs. Our results show that all thirteen ASTs activated Dippu-AstR in a dose dependent manner, albeit with different potencies. Functional analysis of AstR in multiple cell lines demonstrated that activation of the AstR receptor resulted in elevated levels of Ca^{2+} and cAMP, which suggests that Dippu-AstR can act through the $G\alpha_q$ and $G\alpha_s$ protein pathways. The study on the target of AST action reveals that FGL/AST affects JH biosynthesis prior to the entry of acetyl-CoA into the JH biosynthetic pathway.

1. Introduction

Allatostatins (ASTs), a family of pleiotropic neuropeptides, were originally named for their ability to inhibit juvenile hormone (JH) biosynthesis by corpora allata (CA) rapidly and reversibly (Bendena et al., 1999). Three families of ASTs have been identified in insects and named as: FGLa/ASTs (A-type), MIP/ASTs (B-type) and the PISCF/ASTs (C-type) (Coast and Schooley, 2011). The distribution and function of the three families of ASTs has been reviewed by Stay and Tobe (2007). The best documented role of FGLa/AST is their ability to inhibit JH biosynthesis by corpora allata (CA) (Stay and Tobe, 2007). Later studies demonstrated other functions of FGLa/ASTs, including regulation of myotropic activity in gut tissues (Duve et al., 1995; Lange et al., 1995) and cardiac rhythm (Vilaplana et al., 1999), inhibition of vitellogenin synthesis in the fat body (Martin et al., 1996), and stimulation of enzyme activity in the lumen of the midgut (Fuse et al., 1999).

As neuropeptides, ASTs exert their effects by binding to a G protein-coupled receptor, AstR. FGLa/AST receptors, which are structurally related to the mammalian galanin receptor, were first identified in the fly *Drosophila melanogaster* DAR-1 (Birgul et al., 1999) and DAR-2 (Lenz et al., 2000), and later in the silkworm, *Bombyx mori* (Secher et al., 2001) and the stick insect, *Carausius morosus* (Auerswald et al., 2001). In *Diploptera punctata*, putative AstRs have previously been partially characterized using photoaffinity labeling and a radioligand-binding assay in the CA and brain (Cusson et al., 1991; Yu et al., 1995). Lungchukiet et al. (2008b) identified a putative FGLa/AST receptor gene in *D. punctata*. Silencing this gene resulted in a significant increase in JH biosynthesis (Lungchukiet et al., 2008a,b).

The responses of FGLa/AST receptor to FGLa/ASTs have been assayed in *D. melanogaster* (DAR-1 and DAR-2) (Birgul et al., 1999; Larsen et al., 2001), *B. mori* (Secher et al., 2001) and the cockroach, *Periplaneta americana* (Gade et al., 2008). The studies in *B. mori* and *P. americana* focused on the response of AstR to exogenous ASTs. The signaling pathway of AstR was, however, not completely elucidated. Larsen et al. (2001) expressed *Drosophila* FGLa/AST receptors, DAR-1 and DAR-2 in CHO cells and activated them with four putative FGLa/

Abbreviations: AstR, allatostatin receptor; PTX, pertussis toxin; CHO, Chinese hamster ovary; HEK, human embryonic kidney; CRE, cAMP responsive element; AC, adenylate cyclase; MA, mevalonic acid; DPPM, diphosphomevalonate; SEM, standard error of the mean.

* Corresponding author. Department of Cell and Systems Biology, University of Toronto, 25 Harbord Street, Toronto, Ontario, Canada. Tel.: +1 416 978 3517.
E-mail address: stephen.tobe@utoronto.ca (S.S. Tobe).

http://dx.doi.org/10.1016/j.ibmb.2014.09.001
0965-1748/

ASTs from *D. melanogaster* AST and four FGLa/ASTs from *D. punctata* in the presence or absence of pertussis toxin (PTX). They found that PTX caused a complete loss of Ca^{2+} signal in cells expressing DAR-1, and a decreased Ca^{2+} signal in cells expressing DAR-2. Their results suggested that the activation of DAR-1 and DAR-2 by FGLa/ASTs coupled to multiple signaling pathways, including $G_{i/o}$ protein and other, PTX-insensitive G-proteins.

Although the function of AST has been well-studied, little is known about the precise target of AST action. Previous studies focused on select enzymes in the JH biosynthetic pathway. It is now known that thirteen enzymes are involved in the JH biosynthetic pathway (Fig. S1) (Belles et al., 2005; Nouzova et al., 2011). The potential targets of action of ASTs were originally studied by employing different known JH precursors (Pratt et al., 1991, 1989). The results suggested that the inhibitory action of AST on JH biosynthesis resides in step(s) prior to mevalonate. However, neither HMG-CoA synthase nor HMG-CoA reductase activity was affected by ASTs (Sutherland and Feyereisen, 1996). These authors proposed that the target of AST action on JH biosynthesis is located in step(s) prior to the JH biosynthetic pathway, and may be related to the transport of citrate from mitochondria to cytosol and/or to the cleavage of citrate to yield acetyl-CoA.

Our study focuses on the viviparous cockroach, *D. punctata*, in which ASTs were first characterized. The first gonadotropic cycle is characterized by a precise regulation of JH biosynthesis necessary to coordinate a specific series of reproductive events closely correlated with oocyte growth. This makes *D. punctata* an ideal model for a more in depth study of the mode of action of AST and its signal transduction pathway. We have analyzed the spatial expression pattern of the AST precursor and AstR which is consistent with their roles in regulating JH biosynthesis. Moreover, by using an aequorin-based assay and expressing the receptor in a mammalian system, we have unambiguously identified that AST is a ligand for the candidate AstR (Lungchukiet et al., 2008b) and that this receptor can couple to Ca^{2+} and cAMP.

Thirteen FGLa/ASTs have been identified in *D. punctata*. These peptides share a conserved C-terminal Tyr (Phe)–Xaa–Phe–-Gly–Leu–NH_2, which is believed to be the main functional region for the inhibition of JH biosynthesis (Donly et al., 1993; Marchal et al., 2013a). The FGLa/ASTs inhibit JH biosynthesis by CA at low concentrations *in vitro* but with different potencies (Tobe et al., 2000). Our study has also examined the relationship between binding affinity and potency with a view to understanding the sites of action of the peptides.

The precise target of AST action remains unclear so far. Our study did not find any significant changes in the transcript level of genes encoding enzymes in JH biosynthetic pathway. The rescue of AST-induced JH inhibition by JH precursors suggests that the target of AST action is prior to the entry of Acetyl-CoA into the JH biosynthetic pathway.

2. Materials and methods

2.1. Insects

D. punctata were reared in cages and fed with lab chow and water *at libitum* at 27 °C in a dark room. Newly molted female adult cockroaches were picked from the colony and raised in separate containers. Mated status was confirmed by the presence of a spermatophore.

2.2. Tissue collection

Cockroach tissues were dissected under a dissecting microscope. Basal oocyte length was measured to determine the physiological age of cockroaches. Selected tissues were dissected and cleaned in sterile cockroach ringer solution (150 mM NaCl, 12 mM KCl, 10 mM $CaCl_2.2H_2O$, 3 mM $MgCl_2.6H_2O$, 10 mM HEPES, 40 mM Glucose, pH 7.2), and stored at −80 °C to prevent degradation.

2.3. RNA extraction and cDNA synthesis

Pooled samples were homogenized using a plastic pestle and RNA was extracted using the RNeasy Mini Kit (Qiagen) according to the manufacturer's instructions. An additional DNase treatment (RNase-free DNase set, Qiagen) was performed to eliminate potential genomic DNA contamination. RNA of CA was extracted using the RNAqueous®-Micro Kit (Ambion). DNase treatment was performed to eliminate genomic DNA contamination. The quantity and quality of RNA was determined using a Nanodrop spectrophotometer (Thermo Scientific). An equal amount of RNA was transcribed with Superscript III reverse transcriptase (Invitrogen Life Technologies) utilizing random hexamers as described in the protocol. The resulting cDNA was diluted tenfold.

2.4. Quantitative real time-PCR (q-RT-PCR)

Prior to target gene profiling, *Tubulin* and *EF1a* were chosen as the optimal housekeeping genes according to a previous study (Marchal et al., 2013b). The q-RT-PCR reactions were performed in triplicate on a CFX384 Touch™ Real-Time PCR Detection System (Bio-Rad) in a final volume of 10 μl, containing 1 μl of cDNA, 5 μl IQ™ SYBR® Green Supermix (Bio-Rad), 1 μl forward and reverse primer (5 μM) and 2 μl of MQ-water. The reaction was incubated for 3 min in 95 °C, followed by 40 cycles with following thermal profile: 95 °C, 10 s; 59 °C, 30 s. Target specificity was confirmed by running a few representative q-RT-PCR products on an agarose gel containing GelRed™ (Biotium). Realtime primers used for q-RT-PCR are listed in Table S1. Primer sets were validated by determining relative standard curves for each gene transcript using a five-fold serial dilution of a calibrator cDNA sample. Efficiency and correlation coefficient (R^2) are shown in Table S1. The primer sets for genes in the JH biosynthetic pathway were chosen according to Huang et al. (submitted for publication). The quantity of mRNA for each tested gene relative to reference genes was determined as described by Vandesompele et al. (2002).

2.5. Peptides and substrates

Thirteen Dippu-ASTs were custom synthesized by GL Biochemical Ltd., Shanghai (China). Peptides were purified by high performance liquid chromatography (HPLC) (purity ≥95%). Peptides were dissolved in water to obtain a concentration of 1 mM. Peptide solutions were stored at −80 °C prior to further processing and dilution.

Acetyl-CoA, mevalonic acid (MA), diphosphomevalonate (DPPM) and farnesol were purchased from Sigma–Aldrich Canada. Substrates were dissolved in water before use.

2.6. Cell culture and transfection

Chinese hamster ovary (CHO) WTA11 and PAM28 cells stably expressing apoaequorin (Euroscreen, Belgium) and human embryonic kidney (HEK) 293 cells were cultured in monolayers in Dulbecco's Modified Eagles Medium nutrient mixture F12-Ham (DMEM/F12) (Sigma) supplemented with 10% heat-inactivated fetal calf serum (Invitrogen), 100 IU/ml penicillin and 100 μg/ml streptomycin (Invitrogen). An additional 250 μg/ml Zeocin (Invitrogen) was added to the medium for CHO-WTA11 cells, and an additional 5 μg/ml Puromycin (Sigma) was added to the medium

for PAM cells. The cells were cultured at 37 °C with a constant supply of 5% CO_2.

Transfections with pcDNA3.1D-Dippu-AstR or empty pcDNA3.1D vector were carried out in T75 flasks at 60–80% confluency. Transfection medium for CHO cells was prepared using the Lipofectamine LTX kit (Invitrogen) with 3.75 ml Opti-MEM, 7.5 μg vector construct and 18.75 μl Plus™ Reagent in a 5 ml polystyrene round-bottom tube. After 5 min incubation at room temperature, 45 μl LTX (Invitrogen) was added. Transfection medium was added dropwise to the cells after 30 min incubation at room temperature. The transfection medium of the HEK293 cells was similar to that of the CHO cells, except that 9 μg DNA construct (6 μg of vector construct and 3 μg of reporter gene plasmid) was added to the medium. The luciferase ORF, downstream of a cAMP responsive element (CRE) served as the reporter gene. After transfection, cells were incubated overnight and an additional 10 ml of culture medium was added. The cells were allowed to grow for another night prior to intracellular Ca^{2+} or cAMP measurements.

2.7. Aequorin assay

CHO cells were detached using 1 × Phosphate Buffered Saline (PBS) containing 0.2% EDTA (pH 8.0), collected and pelleted by centrifugation in DMEM/F12 medium. The number of viable and nonviable cells was determined using a NucleoCounter NC-100™ (Chemometic). The cells were then resuspended to a density of 5×10^6 cells/ml in sterile filtered DMEM/bovine serum albumin (BSA) medium (DMEM/F12 with L-glutamine and 15 mM HEPES, without Phenol red, supplemented with 0.1% BSA). A concentration of 5 μM coelenterazine h (Invitrogen) was added and the cells were incubated for 4 h in the dark at room temperature with gentle shaking to reconstitute the holo-enzyme aequorin. The cells were then diluted 10-fold in BSA medium and incubated for another 30 min in the dark with gentle shaking. Peptides were dissolved in BSA medium and dispensed in 50 μl aliquots into the wells of a white 96-well plate. Fifty μl of the cell suspension was injected into each well and light emission was recorded using a Mithras LB940 multimode microplate reader (Berthold Technologies) over 30 s. The cells were lysed by injection of 50 μl 0.3% Triton X-100 and light emission was monitored for an additional 8 s. The total response (ligand + Triton-X100) is the representative for the quantity of viable cells present in the well. BSA medium was used as a negative control in each row of the plate, and 1 μM ATP served as a positive control. The negative response was subtracted from the luminescence measured in wells of the same row. Calculations were made using the output file from Microwin software (Berthold Technologies) in Excel (Microsoft). Further analysis was done in Excel and GraphPad Prism 6.

2.8. cAMP reporter assay

HEK cells were detached using 1 × PBS containing 0.2% EDTA (pH 8.0), collected and pelleted by centrifugation in DMEM/F12 medium. The number of viable and nonviable cells was determined using a NucleoCounter NC-100™ (Chemometic). The cells were then resuspended to a concentration of 1×10^6 cells/ml in DMEM/F12 containing 200 μM 3-isobutyl-1-methylxanthine (IBMX, Sigma) to prevent cAMP breakdown. Peptides were dissolved in IBMX medium in the presence or absence of 20 μM forskolin, and were dispensed in 50 μl aliquots into the wells of a white 96-well plate. Fifty μl of cell suspension was added into each well and the plate was incubated in a CO_2 incubator (5% CO_2) at 37 °C for 3.5 h. Fifty μl of Steadylite Plus substrate (PerkinElmer) was then added to each well and the plate was incubated in the dark for 15 min while gently shaking. Light emission resulting from the luciferase enzymatic activity was recorded for 5 s/well using a Mithras LB940. Results were analyzed using the output of MicroWin and further processed by Excel and GraphPad Prism 6.

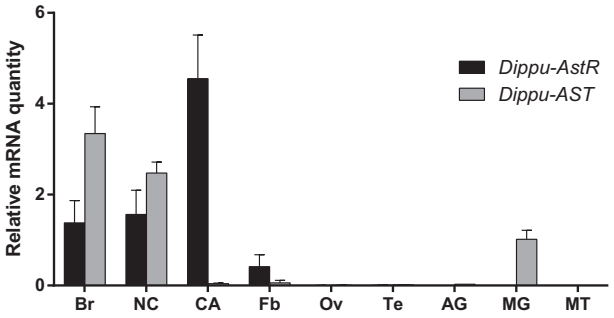

Fig. 1. Relative expression levels of *Dippu-AstR* (black) and *Dippu-AST* (gray) mRNA in tissues of day 4 males and mated females. The data represent averages of 3 pools (10 animals per pool), run in triplicate. Tissues tested are brain (Br), nerve cord (NC), corpora allata (CA), fat body (Fb), ovary (Ov), midgut (MG) and Malpighian tubules (MT) from females and testes (Te) and accessory gland (AG) from males. Values represent mean ± SEM.

2.9. Radiochemical assay (RCA)

The *in vitro* RCA for JH biosynthesis was performed as described by Feyereisen and Tobe (1981) and modified by Tobe and Clarke (1985). Two incubations were conducted in the JH biosynthesis rescue experiments. CA were incubated in TC199 medium with 10^{-6} M AST7 for 3 h, and then transferred to fresh medium with 10^{-6} M AST7 and JH precursors for a second 3 h incubation. JH biosynthesis was determined after each incubation. The rate of JH biosynthesis during the first incubation was used as the control value.

2.10. RNA interference (RNAi)

Dippu-AstR dsRNA constructs were prepared using the MEGAscript® RNAi Kit (Ambion). A 368 bp fragment was amplified by PCR using forward and reverse primers with T7 promoters (TAATACGACTCACTATAGGGAGA) attached to the 5′ end. The sequences for forward and reverse primer were 5′-TGTAATCATACGGCTAACGGATC-3′ and 5′-AATGGTAGAACGTAGTCTGTTGC-3′, respectively. Fragments were subcloned and sequenced to verify the presence of the T7 promoter. The amplified fragment was used in an RNA transcription reaction and incubated overnight to yield annealed dsRNA transcripts. A nuclease digestion was subsequently performed to remove ssRNA and DNA remaining in the product. The dsRNA was further purified according to the manufacturer's instructions (Ambion). Concentration of the dsRNA construct was determined using a nanodrop instrument (Thermo Fisher Scientific Inc.). Five-fold diluted dsRNA was run on a 1.2% agarose gel to examine the quality and integrity of the construct. The control dsRNA was prepared using a PCR fragment amplified from a non-coding region of pJET1.2 cloning vector (Thermo Scientific).

Dippu-AstR dsRNA was diluted in cockroach saline to a concentration of 250 ng/μl. Each adult female was injected with 4 μl of dsRNA solution on day 0, 2 and 4 after the final moult. CA were dissected on day 6 and stored in liquid nitrogen prior to RNA extraction. A second set of cockroaches was injected with *Dippu-AstR* dsRNA in the same scheme as described above. CA were dissected on day 6 and cleaned in TC199 medium (GIBCO; 1.3 mM Ca^{2+}, 2% Ficoll, methionine-free) for their use in the radiochemical assay (RCA) determining the effect of AST on JH biosynthesis. Basal oocyte length was measured during dissection.

3. Results

3.1. Tissue distribution of Dippu-AST and Dippu-AstR

The tissue distribution of *Dippu-AST* and *Dippu-AstR* was determined in adult male and female cockroaches using q-RT-PCR (Fig. 1). Nine tissues were used to examine the tissue specificity of *Dippu-AST* and *Dippu-AstR*: brain (Br), nerve cord (NC), corpora allata (CA), fat body (Fb), ovary (Ov), midgut (MG) and Malpighian tubules (MT) from females and accessory gland (AG) and testes (Te) from males. The *Dippu-AST* gene is expressed in brain, nerve cord and midgut, which is consistent with the pleiotropic functions of ASTs (Fig. 1). *Dippu-AstR* shows the highest transcription levels in the CA, followed by nerve cord, brain and fat body. All the other tissues tested showed either negligible or undetectable levels of *Dippu-AstR* mRNA.

3.2. Functional activation of Dippu-AstR with ASTs

We initially expressed Dippu-AstR in CHO-WTA11 cells. This cell line expresses the Ca^{2+} reporter apoaequorin and $G\alpha_{16}$, a promiscuous G protein that couples to most GPCRs with subsequent mobilization of intracellular Ca^{2+} (Stables et al., 1997). As shown in Fig. 2, all 13 tested ASTs induced clear dose-dependent bioluminescence responses in AstR expressing cells. Most of the peptides showed similar degrees of biological efficacy (ability to activate AstR) but differed considerably in potency, with EC_{50} values ranging from 0.2 nM for AST6 to 30 nM, in the case of AST13 (Table 1). In general, the abilities of ASTs to activate AstR corresponded to their potencies as inhibitors of JH production by the CA, with the exception of AST1, AST5 and AST6 (Tobe et al., 2000) (Table 1).

To determine the second messenger pathways involved in Dippu-AstR activation, we first expressed Dippu-AstR in CHO-PAM28 cells (lacking the promiscuous $G\alpha_{16}$). The expression of apoaequorin in the cell allows testing whether the receptor can couple naturally through intracellular Ca^{2+}. Two ASTs (AST5 and 6) were chosen because of their high potency in inhibiting JH biosynthesis or in activating Dippu-AstR. As shown in Fig. 3A, AST5 and 6 induced dose-dependent intracellular Ca^{2+} responses in AstR-transfected CHO-PAM28 cells, with EC_{50} values of 21.4 nM and 1.1 nM, respectively.

We subsequently tested whether the receptor coupled with cAMP in the signal transduction pathway. We expressed Dippu-AstR in HEK293 cells, which contain the luciferase gene under the control of a cAMP response element. We assayed different concentrations of AST5 and AST6 in the presence or absence of forskolin. Forskolin activates adenylate cyclase (AC), which increases intracellular levels of cAMP. If AstR would couple negatively to AC, we would expect lower levels of cAMP following application of ASTs. This was not the case. Application of AST5 or AST6 to

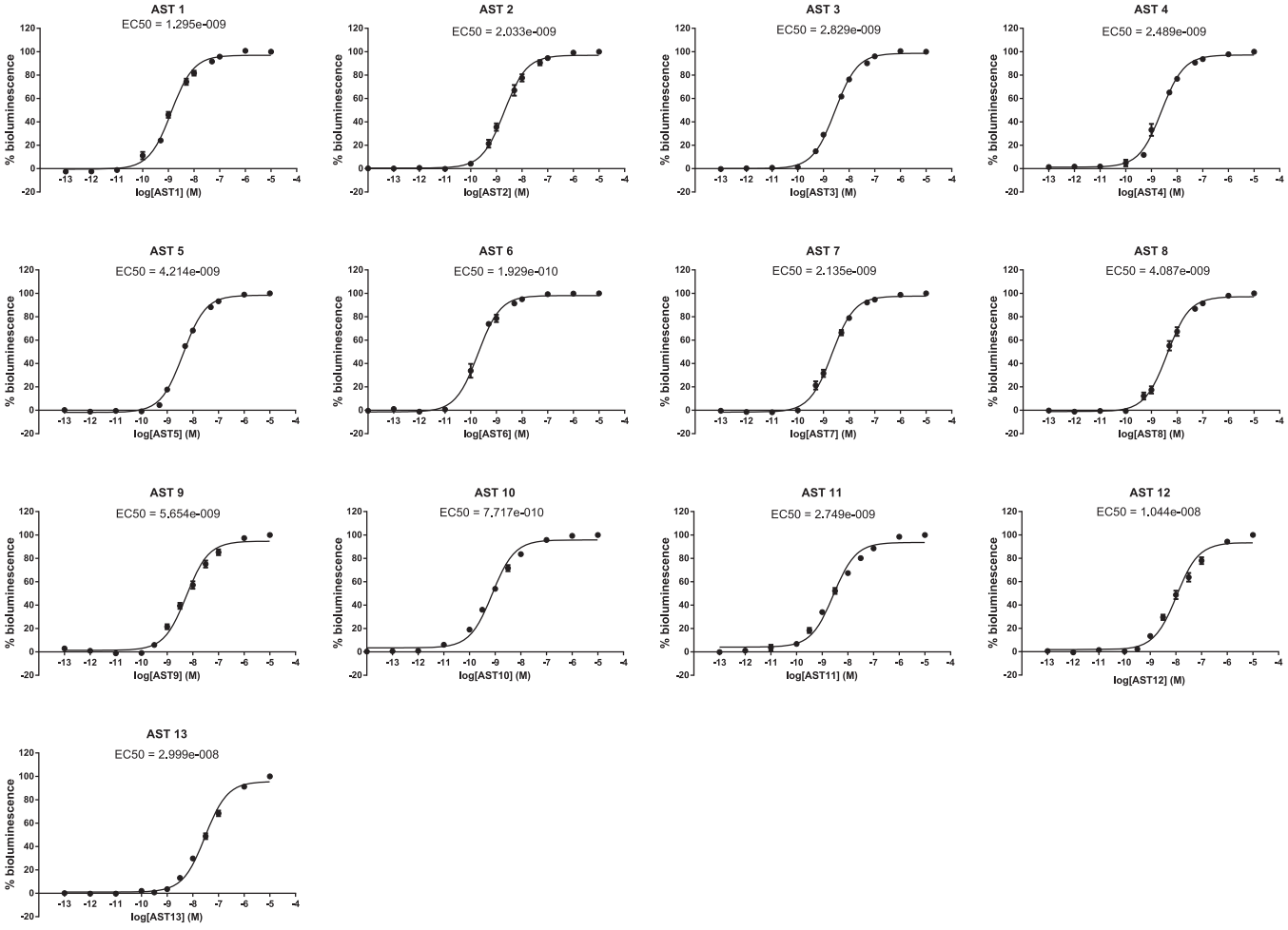

Fig. 2. Dose–response curves for ASTs in CHO-WTA11 cells expressing Dippu-AstR. Data points represent the average ± SEM of three independent measurements performed in duplicate and are expressed as percentage of the maximal response. The zero response level corresponds to treatment with BSA buffer only.

Table 1
Potency of Dippu-ASTs[a]: activation of AstR in CHO-WTA11 cells (EC_{50}) or inhibitory effect on JH release (IC_{50}).

Allatostatin	EC_{50}[b]/nM	Rank[b] order (EC_{50})	IC_{50}[c]/nM	Rank[c] order (IC_{50})	Sequence
AST1	**1.295**	**3**	9.566	11	Leu–Tyr–Asp–Phe–Gly–Leu–NH2
AST2	**2.033**	**4**	0.4254	3	Ala–Tyr–Ser–Tyr–Val–Ser–Glu–Tyr–Lys–Arg–Leu–Pro–Val–Tyr–Asn–Phe–Gly–Leu–NH2
AST3	**2.829**	**8**	12.54	12	Ser–Lys–Met–Tyr–Gly–Phe–Gly–Leu–NH2
AST4	**2.489**	**6**	1.139	5	Asp–Gly–Arg–Met–Tyr–Ser–Phe–Gly–Leu–NH2
AST5	**4.214**	**10**	0.1063	1	Asp–Arg–Leu–Tyr–Ser–Phe–Gly–Leu–NH2
AST6	**0.1929**	**1**	2.725	8	Ala–Arg–Pro–Tyr–Ser–Phe–Gly–Leu–NH2
AST7	**2.135**	**5**	0.4118	2	Ala–Pro–Ser–Gly–Ala–Gln–Arg–Leu–Tyr–Gly–Phe–Gly–Leu–NH2
AST8	**4.087**	**9**	3.275	10	Gly–Gly–Ser–Leu–Tyr–Ser–Phe–Gly–Leu–NH2
AST9	**5.654**	**11**	2	6	Gly–Asp–Gly–Arg–Leu–Tyr–Ala–Phe–Gly–Leu–NH2
AST10	**0.7717**	**2**	0.9225	4	Pro–Val–Asn–Ser–Gly–Arg–Ser–Ser–Gly–Ser–Arg–Phe–Asn–Phe–Gly–Leu–NH2
AST11	**2.749**	**7**	2.795	9	Tyr–Pro–Gln–Glu–His–Arg–Phe–Ser–Phe–Gly–Leu–NH2
AST12	**10.44**	**12**	2.011	7	Pro–Phe–Asn–Phe–Gly–Leu–NH2
AST13	**29.99**	**13**	12.84	13	Ile–Pro–Met–Tyr–Asp–Phe–Gly–Ile–NH2

[a] Potency is defined as the dose required to achieve a given level of activation of AstR or inhibition of JH biosynthesis, and is listed in rank order.
[b] EC_{50} was determined by AstR activation assay in CHO-WTA11 cells (details seen Fig. 1) with values from the present study shown in bold..
[c] IC_{50} values are as reported by Tobe et al. (2000) (CA from day 2 virgin female).

transfected HEK cells did not cause any significant change in cAMP level. However, in the absence of forskolin, AST5 and AST6 treatments resulted in a dose-dependent increase in cAMP concentration, as measured by assay of luciferase activity (Fig. 3B). The EC_{50} values were 287.8 nM for AST5 and 24.3 nM for AST6. The EC_{50} values for the cAMP-based luciferase assay in HEK293 cells were higher than for the Ca^{2+} responses detected in either of the two CHO cell lines, but the relative order of ligand potency was maintained. CHO-WTA11, CHO-PAM28 and HEK293 cells transfected with pcDNA3.1D (empty vector) did not show any response to ASTs.

3.3. AST does not affect the transcript level of enzymes in the JH biosynthetic pathway

The injection of *AstR* dsRNA on days 0, 2 and 4 resulted in a 67% knockdown of *AstR* mRNA levels in CA of day 6 females (Fig. 4A). The JH biosynthetic activity of CA was measured using the RCA. In *AstR* knockdown animals, JH production increased by 60% and the response of CA to AST decreased by 28% (Fig. 4B and C). Eleven of 13 genes encoding enzymes in the JH biosynthetic pathway have been identified (Huang et al., submitted for publication). To determine the target of AST action in the JH biosynthetic pathway, we measured the mRNA levels of the 11 genes encoding enzymes catalyzing different steps in the JH biosynthetic pathway. Although *AstR* dsRNA treatment resulted in an increase in the rate of JH biosynthesis, none of the relative transcript levels showed significant changes (Fig. 4D). The high variation of the transcript level of *JHAMT* on day 6 can be explained by previous results that show a great degree of fluctuation in *JHAMT* mRNA levels at times when rates of JH biosynthesis are highly dynamic (Huang et al., submitted for publication).

To confirm our results, we incubated CA in medium containing 10^{-7} M AST7 for 3 h, which results in a 60–70% decrease in JH biosynthesis (Tobe et al., 2000), and determined the transcript level of the enzymes in the CA. As in the *AstR* RNAi experiments, the mRNA levels of the 11 genes tested show no significant changes (Fig. 5).

3.4. JH precursors reverse AST-induced inhibition of JH biosynthesis

Earlier studies showed that mevalonate and farnesol were able to partially reverse AST-induced inhibition of JH biosynthesis (Pratt et al., 1991, 1989). To determine which enzyme(s) is/are affected by ASTs in the JH biosynthetic pathway, we treated CA with select JH precursors in the presence of 10^{-6} M AST7. If the activity of enzymes was inhibited by AST, the JH precursors prior to the enzyme will not be able to reverse the inhibition of AST. As shown in Fig. 6, all exogenous JH precursors acetyl-CoA, mevalonic acid, diphosphomevalonate and farnesol significantly stimulated the rate of JH biosynthesis in the presence of AST7 (Fig. 6).

4. Discussion

Our observations on the expression of the *Dippu-AstR* and *Dippu-AST* provide insights into the tissue-specific interaction between the ligands and the receptor. In brain and nerve cord, both

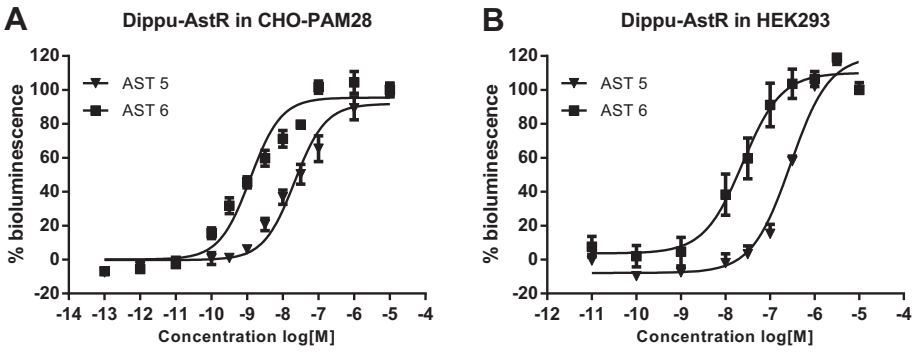

Fig. 3. Dose–response curves for the bioluminescence response induced in (A) CHO-PAM28 and (B) HEK293 cells expressing Dippu-AstR. Data points represent the average ± SEM of three independent measurements performed in duplicate and are expressed as a percentage of the maximal response. The zero response level corresponds to treatment with BSA buffer only. Peptides tested are AST5 (squares) and AST6 (triangles).

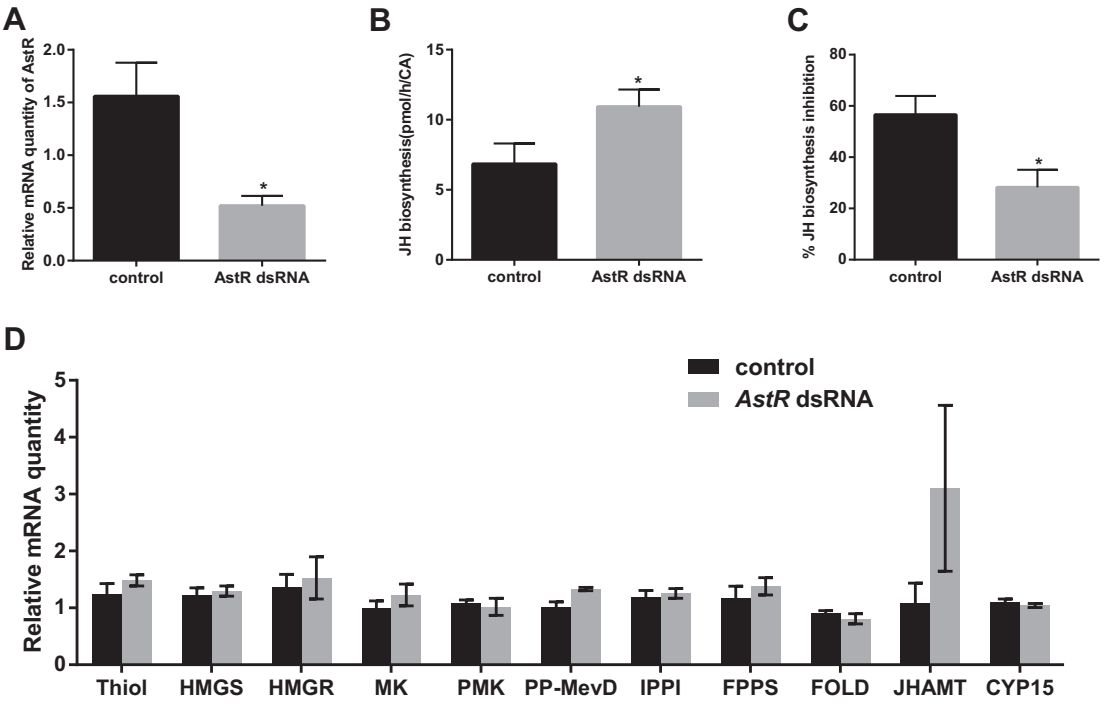

Fig. 4. The effect of *Dippu-AstR* dsRNA on JH biosynthesis by the CA and on the expression of genes encoding enzymes in the JH biosynthetic pathway of *D. punctata*. (A) Efficiency of *Dippu-AstR* RNAi-mediated knockdown in mated females. Relative quantity of *Dippu-AstR* mRNA levels in CA was compared between control and *AstR* dsRNA treated animals. (B) JH biosynthesis by CA from *Dippu-AstR* dsRNA-treated animals. Glands were taken from day 6 mated females, $n \geq 10$. (C) Effect of 10^{-7} M Dippu-AST7 on JH biosynthesis by CA from control and *AstR* knockdown animals. CA were incubated first in normal medium for 3 h and subsequently incubated in medium with 10^{-7} M AST7 for another 3 h. The percentage of inhibition was calculated using the rate of JH biosynthesis during the first and second incubation. (D) The effect of silencing *Dippu-AstR* on the transcript levels of genes encoding enzymes in the JH biosynthetic pathway. Enzyme abbreviations are as described in Figure S1. The mRNA quantity data represent averages of 3 pools (8 pairs of CA per pool) run in triplicates using q-RT-PCR. Vertical bars indicate SEM. Significant differences are indicated by asterisks ($^{*}P < 0.05$).

Dippu-AstR and *Dippu-AST* are expressed, whereas in CA, only the receptor is expressed. This is in consistent with observations that AST is delivered to the CA by nerves from neurosecretory cells in the brain (Stay et al., 1992). In the midgut, however, *Dippu-AST* is expressed, but its receptor is not (Fig. 1); tissue distribution of *Dippu-AstR* and *Dippu-AST* in day 7 animals provided similar results (Fig. S2). Previous studies suggest that ASTs can induce myotropic activity in gut tissues (Duve et al., 1995; Lange et al., 1995). Furthermore, putative receptors for ASTs in midgut were partially characterized using a radioligand-binding assay (Bowser and Tobe, 2000). Therefore, the undetectable transcript level of *Dippu-AstR* in midgut suggests that one or more additional AstR in *D. punctata* may exist, just as two receptors for allatostatins have been identified in *D. melanogaster* (Birgul et al., 1999; Lenz et al., 2000).

To functionally analyze AstR, we expressed the Dippu-AstR in mammalian cells and activated it with Dippu-AST. We first expressed Dippu-AstR in CHO cells, demonstrating that it is indeed a *Diploptera* allatostatin receptor. All thirteen ASTs are very potent in activating AstR expressed in CHO-WTA11 cells with EC_{50} values in the low nanomolar range (Fig. 2). Despite the structural similarities, there were some differences in the response to individual peptides. AST13, which contains isoleucine at the C-terminus, exhibited the highest EC_{50}. This result reinforces the importance of the C-terminal pentapeptide motif Y/FXFGL-NH_2. Moreover, the amino acids outside of the C-terminal pentapeptide motif appear to determine the affinity of AST for AstR as well. AST5 and AST6 have the same pentapeptide motif (Table 1), whereas their ability to activate the receptor is significantly different. The change of Pro to Leu, and Ala to Asp decreases AST affinity of AstR by 20-fold.

The rank order of potency of Dippu-ASTs in activating Dippu-AstR expressed in CHO-WTA11 cells is similar to that for the *P. americana* receptor (Gade et al., 2008). However, the potencies of AST 1, 5 and 6

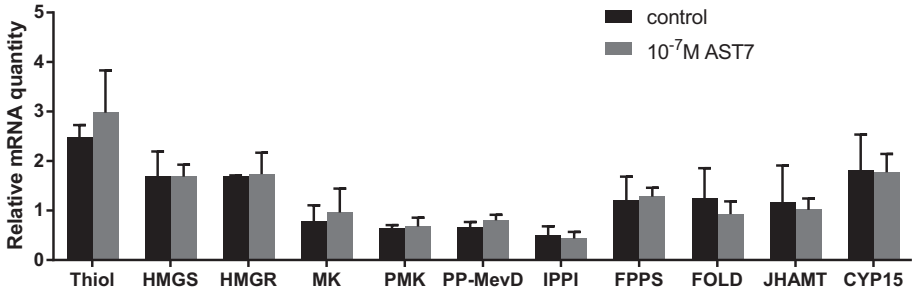

Fig. 5. The effect of AST on the expression levels of genes encoding enzymes in the JH biosynthetic pathway in CA of day 6 mated female *D. punctata*. CA were incubated for 3 h in normal (control) medium or medium supplemented with 10^{-7} M AST7 (treatment) and then washed with cockroach saline prior to the RNA extraction. RNA was extracted from CA in control and treatment groups to determine the transcript level of genes encoding enzymes in JH biosynthetic pathway. Enzyme abbreviations are as described in Figure S1. The data represent averages of 3 pools (8 pairs of CA per pool) run in triplicate using q-RT-PCR. Vertical bars indicate SEM.

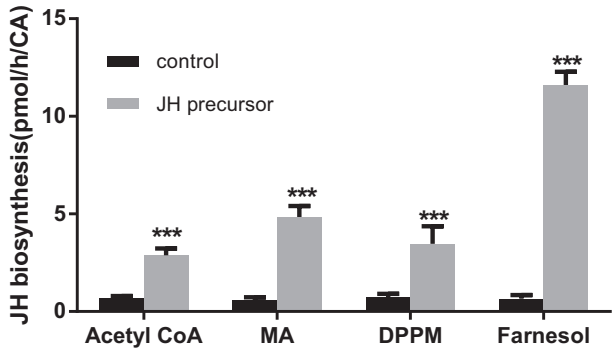

Fig. 6. JH precursors rescue the AST-induced JH inhibition. JH biosynthesis was evaluated in CA that were first incubated in medium TC199 with 10^{-6} M AST7 (control), and then in medium with 10^{-6} M AST7 together with the individual precursors: Acetyl-CoA (100 μM), MA (100 μM), DPPM (100 μM) or farnesol (40 μM). CA were dissected from day 7 mated females. Each data point represents mean ± SEM ($n \geq 10$).

in activating AstR differ from their capacities to inhibit JH production *in vitro* (Table 1). AST 5, which showed the highest inhibitory activity, demonstrated only a moderate potency in activating the expressed Dippu-AstR, ranking 10 out of 13. In contrast, AST1, which was one of the weakest inhibitors of JH biosynthesis *in vitro* (ranking 11 out of 13), appears to be one of the most potent peptides in receptor activation. AST6, the structure of which is conserved in several insect orders, showed the highest potency in activating expressed Dippu-AstR (Bendena et al., 1999). Its ability to inhibit JH biosynthesis, on the other hand, was moderate. Different reasons could contribute to the differences between potency in activating the receptor and inhibiting JH biosynthesis *in vitro*. The susceptibility of ASTs to degradation by enzymes in the CA differs between ASTs, which could result in different potencies in inhibiting JH biosynthesis. AST5, which showed high resistance to the degradation by hemolymph and membrane preparations, presented the highest activity in inhibiting JH biosynthesis (Garside et al., 1997a,b). Furthermore, tests with cloned receptors in mammalian cells might not fully reflect the actual situation in insects. The posttranslational modifications of AstR or the interacting proteins present in receptor-expressing cells could affect the conformational and functional properties of this receptor. Nevertheless, we here chose mammalian cell lines because there may be fewer interacting proteins in this heterologous system than in insect cell lines.

The inhibition of JH biosynthesis by Dippu-ASTs is a complex process, probably involving more than one second messenger. Previous studies showed that ASTs regulate JH biosynthesis by acting through the inositol trisphosphate (IP_3)/diglyceride (DAG) second messenger systems, in which protein kinase C (PKC) and Ca^{2+} are involved (Feyereisen and Farnsworth, 1987b; Rachinsky and Tobe, 1996; Rachinsky et al., 1994). However, the role of Ca^{2+} in regulation of JH biosynthesis is confounding. JH production shows dose-dependency on extracellular Ca^{2+} in the medium, whereas the Ca^{2+} ionophore A23187 caused a rapid decline in JH release (Kikukawa et al., 1987). Inhibition of JH biosynthesis by brain extracts was antagonized by inorganic Ca^{2+}channel blockers (Feyereisen and Farnsworth, 1987a). However, elevation of intracellular Ca^{2+} levels by treating CA with the Ca^{2+}-mobilizing drug thapsigargin diminished the inhibitory effect of ASTs (Rachinsky et al., 1994). The activation of Dippu-AstR induced a dose-dependent intracellular Ca^{2+} response in CHO-PAM28 cells (Fig. 3A), which supports the involvement of Ca^{2+} as a second messenger of AST. Aucoin et al. (1987) suggested that there may be both a Ca^{2+}-dependent and a Ca^{2+}-independent pathway (cAMP) involved in the inhibition of JH biosynthesis. Incubating CA with brain extracts resulted in an increase in the level of cAMP and a decrease in JH biosynthesis (Aucoin et al., 1987). Forskolin, which causes a dose-dependent accumulation of cAMP, led to a rapid and dose-dependent inhibition of JH biosynthesis. Moreover, the sensitivity of CA to forskolin shows the same pattern as its sensitivity to AST during the first gonadotrophic cycle (Feyereisen and Farnsworth, 1987a; Meller et al., 1985). In contrast, Cusson et al. (1992) suggest that levels of cAMP do not increase following treatment of CA with ASTs. Our findings demonstrated that the activation of Dippu-AstR induced a dose-dependent cAMP response in HEK293 cells, which suggests that cAMP may be involved in the signaling pathway of AST cells (Fig. 3B). Dippu-AstR appears to dually couple through the $G\alpha_s$ and $G\alpha_q$ pathways and triggers the release of intracellular Ca^{2+} and the increase in cAMP levels. Studies on *Drosophila* AstRs suggested that DAR-1 and DAR-2 couple to $G_{i/o}$ mediated signaling and other G-proteins (Birgul et al., 1999; Larsen et al., 2001). However, activation of AstR in the presence of forskolin did not significantly influence the cAMP signal. This result suggests that there is no involvement of $G\alpha_i$ in the Dippu-AstR pathway.

AST regulates JH biosynthesis by affecting either enzymes directly involved in the JH biosynthetic pathway or steps prior to the production of acetyl-CoA. We have studied the effect of AST on the transcript levels of genes in the JH biosynthetic pathway. The inhibitory effect of AST on JH biosynthesis was rapid and reversible, which suggests that AST may not regulate JH biosynthesis through transcript levels (Pratt et al., 1991, 1989). Our study confirmed this earlier assumption by revealing that the transcript levels of genes in the JH biosynthetic pathway were not affected by *AstR* silencing or AST treatment *in vitro* (Figs. 4 and 5). Previous studies indicate that ASTs regulate JH biosynthesis through steps(s) prior to the production of mevalonate (Pratt et al., 1991, 1989). However, the enzyme activities of HMG-CoA synthase or HMG-CoA reductase were not affected by AST (Sutherland and Feyereisen, 1996). To determine which enzyme in the JH biosynthetic pathway was influenced by AST, we used several JH precursors to reverse the AST-induced inhibition of JH biosynthesis. All the JH precursors (including acetyl-CoA) were able to partially restore JH biosynthesis, thereby suggesting that the enzyme activities were not affected by AST. The target of AST action probably lies prior to the start of the JH biosynthetic pathway in regulating the production of precursors of acetyl-CoA such as the transport of citrate from mitochondria to cytosol and/or the cleavage of citrate to yield acetyl-CoA (Sutherland and Feyereisen, 1996). Further investigation is needed to identify the exact target of AST.

5. Conclusion

In *D. punctata*, ASTs play an important role in the regulation of JH biosynthesis. The potency of the 13 ASTs in activating AstR reveals the structure–activity relationship of AST action. The activation of AstR in CHO and HEK cells suggests that both Ca^{2+} and cAMP can be involved in the signal transduction of AST. Our results show that AST does not affect the transcript levels and that the activities of enzymes in the JH biosynthetic pathway remain normal following treatment with AST. AST probably affects JH biosynthesis prior to the entry of precursors into the JH biosynthetic pathway. The exact target of AST action remains an open question.

Acknowledgments

The authors are very grateful to Dr. Jennifer Mitchell for use of the q-RT-PCR equipment and to Dr. William G. Bendena and Dr. Heleen Verlinden for technical assistance on AstR cell expression. The authors also thank the Natural Sciences and Engineering Research Council of Canada RGPIN 9408-09 to SST, China Scholarship Council Doctoral Award, the Interuniversity Attraction Poles

Program (Belgian Science Policy Grant P7/40) and the KU Leuven Research Foundation (GOA/11/02) for financial support.

Appendix A. Supplementary material

Supplementary data related to this article can be found at http://dx.doi.org/10.1016/j.ibmb.2014.09.001.

References

Aucoin, R.R., Rankin, S.M., Stay, B., Tobe, S.S., 1987. Calcium and cyclic-AMP involvement in the regulation of juvenile hormone biosynthesis in *Diploptera punctata*. Insect Biochem. 17, 965–969.

Auerswald, L., Birgul, N., Gade, G., Kreienkamp, H.J., Richter, D., 2001. Structural, functional, and evolutionary characterization of novel members of the allatostatin receptor family from insects. Biochem. Biophys. Res. Commun. 282, 904–909.

Belles, X., Martin, D., Piulachs, M.D., 2005. The mevalonate pathway and the synthesis of juvenile hormone in insects. Annu. Rev. Entomol. 50, 181–199.

Bendena, W.G., Donly, B.C., Tobe, S.S., 1999. Allatostatins: a growing family of neuropeptides with structural and functional diversity. Ann. N. Y. Acad. Sci. 897, 311–329.

Birgul, N., Weise, C., Kreienkamp, H.J., Richter, D., 1999. Reverse physiology in *Drosophila*: identification of a novel allatostatin-like neuropeptide and its cognate receptor structurally related to the mammalian somatostatin/galanin/opioid receptor family. EMBO J. 18, 5892–5900.

Bowser, P.R.F., Tobe, S.S., 2000. Partial characterization of a putative allatostatin receptor in the midgut of the cockroach *Diploptera punctata*. Gen. Comp. Endocrinol. 119, 1–10.

Coast, G.M., Schooley, D.A., 2011. Toward a consensus nomenclature for insect neuropeptides and peptide hormones. Peptides 32, 620–631.

Cusson, M., Prestwich, G.D., Stay, B., Tobe, S.S., 1991. Photoaffinity-labeling of allatostatin receptor proteins in the corpora allata of the cockroach, *Diploptera punctata*. Biochem. Biophys. Res. Commun. 181, 736–742.

Cusson, M., Yagi, K.J., Guan, X.C., Tobe, S.S., 1992. Assessment of the role of cyclic-nucleotides in allatostatin-induced inhibition of juvenile hormone biosynthesis in *Diploptera punctata*. Mol. Cell. Endocrinol. 89, 121–125.

Donly, B.C., Ding, Q., Tobe, S.S., Bendena, W.G., 1993. Molecular cloning of the gene for the allatostatin family of neuropeptides from the cockroach *Diploptera punctata*. Proc. Natl. Acad. Sci. U. S. A. 90, 8807–8811.

Duve, H., Wren, P., Thorpe, A., 1995. Innervation of the foregut of the cockroach *Leucophaea maderae* and inhibition of spontaneous contractile activity by callatostatin neuropeptides. Physiol. Entomol. 20, 33–44.

Feyereisen, R., Farnsworth, D.E., 1987a. Comparison of the inhibitory effects of brain extract, high K+ and forskolin on juvenile hormone synthesis by *Diploptera punctata* corpora allata. Insect Biochem. 17, 939–942.

Feyereisen, R., Farnsworth, D.E., 1987b. Inhibition of insect juvenile hormone synthesis by phorbol 12-myristate 13-acetate. FEBS Lett. 222, 345–348.

Feyereisen, R., Tobe, S.S., 1981. A rapid partition assay for routine analysis of juvenile hormone release by insect corpora allata. Anal. Biochem. 111, 372–375.

Fuse, M., Zhang, J.R., Partridge, E., Nachman, R.J., Orchard, I., Bendena, W.G., Tobe, S.S., 1999. Effects of an allatostatin and a myosuppressin on midgut carbohydrate enzyme activity in the cockroach *Diploptera punctata*. Peptides 20, 1285–1293.

Gade, G., Marco, H.G., Richter, D., Weaver, R.J., 2008. Structure–activity studies with endogenous allatostatins from *Periplaneta americana*: expressed receptor compared with functional bioassay. J. Insect Physiol. 54, 988–996.

Garside, C.S., Hayes, T.K., Tobe, S.S., 1997a. Degradation of Dip-allatostatins by hemolymph from the cockroach, *Diploptera punctata*. Peptides 18, 17–25.

Garside, C.S., Hayes, T.K., Tobe, S.S., 1997b. Inactivation of Dip-allatostatin 5 by membrane preparations from the cockroach *Diploptera punctata*. Gen. Comp. Endocrinol. 108, 258–270.

Huang, J., Marchal, E., Hult, E.F., Tobe, S.S., Characterization of the Juvenile Hormone pathway in the viviparous cockroach, *Diploptera punctata*, (Submitted for publication).

Kikukawa, S., Tobe, S.S., Solowiej, S., Rankin, S.M., Stay, B., 1987. Calcium as a regulator of juvenile hormone biosynthesis and release in the cockroach *Diploptera punctata*. Insect Biochem. 17, 179–187.

Lange, A.B., Bendena, W.G., Tobe, S.S., 1995. The effect of the 13 Dip-allatostatins on myogenic and induced contractions of the cockroach (*Diploptera punctata*) hindgut. J. Insect Physiol. 41, 581–588.

Larsen, M.J., Burton, K.J., Zantello, M.R., Smith, V.G., Lowery, D.L., Kubiak, T.M., 2001. Type A allatostatins from *Drosophila melanogaster* and *Diploptera punctata* activate two *Drosophila* allatostatin receptors, DAR-1 and DAR-2, expressed in CHO cells. Biochem Biophys. Res. Commun. 286, 895–901.

Lenz, C., Williamson, M., Grimmelikhuijzen, C.J.P., 2000. Molecular cloning and genomic organization of a second probable allatostatin receptor from *Drosophila melanogaster*. Biochem. Biophys. Res. Commun. 273, 571–577.

Lungchukiet, P., Donly, B.C., Zhang, J.R., Tobe, S.S., Bendena, W.G., 2008a. Molecular cloning and characterization of an allatostatin-like receptor in the cockroach *Diploptera punctata*. Peptides 29, 276–285.

Lungchukiet, P., Zhang, J.R., Tobe, S.S., Bendena, W.G., 2008b. Quantification of allatostatin receptor mRNA levels in the cockroach, *Diploptera punctata*, using real-time PCR. J. Insect Physiol. 54, 981–987.

Marchal, E., Hult, E.F., Huang, J., Stay, B., Tobe, S.S., 2013a. *Diploptera punctata* as a model for studying the endocrinology of arthropod reproduction and development. Gen. Comp. Endocrinol. 188, 85–93.

Marchal, E., Hult, E.F., Huang, J., Tobe, S.S., 2013b. Sequencing and validation of housekeeping genes for quantitative real-time PCR during the gonadotrophic cycle of *Diploptera punctata*. BMC Res. Notes 6, 237–246.

Martin, D., Piulachs, M.D., Belles, X., 1996. Inhibition of vitellogenin production by allatostatin in the German cockroach. Mol. Cell. Endocrinol. 121, 191–196.

Meller, V.H., Aucoin, R.R., Tobe, S.S., Feyereisen, R., 1985. Evidence for an inhibitory role of cyclic-AMP in the control of juvenile hormone biosynthesis by cockroach corpora allata. Mol. Cell. Endocrinol. 43, 155–163.

Nouzova, M., Edwards, M.J., Mayoral, J.G., Noriega, F.G., 2011. A coordinated expression of biosynthetic enzymes controls the flux of juvenile hormone precursors in the corpora allata of mosquitoes. Insect Biochem. Mol. Biol. 41, 660–669.

Pratt, G.E., Farnsworth, D.E., Fok, K.F., Siegel, N.R., McCormack, A.L., Shabanowitz, J., Hunt, D.F., Feyereisen, R., 1991. Identity of a second type of allatostatin from cockroach brains: an octadecapeptide amide with a tyrosine-rich address sequence. Proc. Natl. Acad. Sci. U. S. A. 88, 2412–2416.

Pratt, G.E., Farnsworth, D.E., Siegel, N.R., Fok, K.F., Feyereisen, R., 1989. Identification of an allatostatin from adult *Diploptera punctata*. Biochem. Biophys. Res. Commun. 163, 1243–1247.

Rachinsky, A., Tobe, S.S., 1996. Role of second messengers in the regulation of juvenile hormone production in insects, with particular emphasis on calcium and phosphoinositide signaling. Arch. Insect Biochem. Physiol. 33, 259–282.

Rachinsky, A., Zhang, J., Tobe, S.S., 1994. Signal transduction in the inhibition of juvenile hormone biosynthesis by allatostatins – roles of diacylglycerol and calcium. Mol. Cell. Endocrinol. 105, 89–96.

Secher, T., Lenz, C., Cazzamali, G., Sorensen, G., Williamson, M., Hansen, G.N., Svane, P., Grimmelikhuijzen, C.J.P., 2001. Molecular cloning of a functional allatostatin gut/brain receptor and an allatostatin preprohormone from the silkworm *Bombyx mori*. J. Biol. Chem. 276, 47052–47060.

Stables, J., Green, A., Marshall, F., Fraser, N., Knight, E., Sautel, M., Milligan, G., Lee, M., Rees, S., 1997. A bioluminescent assay for agonist activity at potentially any G protein-coupled receptor. Anal. Biochem. 252, 115–126.

Stay, B., Chan, K.K., Woodhead, A.P., 1992. Allatostatin-immunoreactive neurons projecting to the corpora allata of adult *Diploptera punctata*. Cell Tissue Res. 270, 15–23.

Stay, B., Tobe, S.S., 2007. The role of allatostatins in juvenile hormone synthesis in insects and crustaceans. Annu. Rev. Entomol. 52, 277–299.

Sutherland, T.D., Feyereisen, R., 1996. Target of cockroach allatostatin in the pathway of juvenile hormone biosynthesis. Mol. Cell. Endocrinol. 120, 115–123.

Tobe, S.S., Clarke, N., 1985. The effect of L-methionine concentration on juvenile hormone biosynthesis by corpora allata of the cockroach *Diploptera punctata*. Insect Biochem. 15, 175–179.

Tobe, S.S., Zhang, J.R., Bowser, P.R., Donly, B.C., Bendena, W.G., 2000. Biological activities of the allatostatin family of peptides in the cockroach, *Diploptera punctata*, and potential interactions with receptors. J. Insect Physiol. 46, 231–242.

Vandesompele, J., De Preter, K., Pattyn, F., Poppe, B., Van Roy, N., De Paepe, A., Speleman, F., 2002. Accurate normalization of real-time quantitative RT-PCR data by geometric averaging of multiple internal control genes. Genome Biol. 3. RESEARCH0034.

Vilaplana, L., Maestro, J.L., Piulachs, M.D., Belles, X., 1999. Modulation of cardiac rhythm by allatostatins in the cockroach *Blattella germanica* (L.) (Dictyoptera, Blattellidae). J. Insect Physiol. 45, 1057–1064.

Yu, C.G., Hayes, T.K., Strey, A., Bendena, W.G., Tobe, S.S., 1995. Identification and partial characterization of receptors for allatostatins in brain and corpora allata of the cockroach *Diploptera punctata* using a binding assay and photoaffinity-labeling. Regul. Pept. 57, 347–358.